Latency-Control Tradeoffs in Communication-Control Co-Designed Networks

Songita Das*, Gourab Ghatak§, Chen Quan†, and Geethu Joseph†

*Bharti School of Telecommunication Technology and Management, Indian Institute of Technology Delhi, India
§Department of Electrical Engineering, Indian Institute of Technology Delhi, India
†Faculty of Electrical Engineering, Mathematics, and Computer Science, Delft University of Technology, Netherlands
Email: bsz228102@iitd.ac.in, gghatak@ee.iitd.ac.in, c.quan@tudelft.nl, g.joseph@tudelft.nl

***Abstract*—We investigate communication-control co-design for wireless networked control systems with block-structured transmissions. Controllers are spatially distributed according to a Poisson point process. They communicate with actuators over an interference-limited wireless channel using probabilistic channel access. Using stochastic geometry, we derive block controllability of the system through run-length analysis of Bernoulli transmission outcomes. To capture temporal reliability, we introduce the concept of peak control latency. It is defined as the number of blocks between consecutive controllable blocks, and we derive its distribution. Finally, we develop an optimization framework that adapts block and slot channel access probabilities to balance controllability and latency. Numerical results demonstrate the trade-off between controllability and latency and show the effectiveness of our adaptive access strategy.**

***Index Terms*—Wireless control-communication co-design, latency, controllability, stochastic geometry.**

I. Introduction

From factory automation and driverless car fleets to Internet-of-Things deployments, wireless networked control systems are ubiquitous. These systems require reliable communication to achieve controllability [1] and maintain temporal consistency in control performance. In particular, controllability depends on consecutive successful transmissions [1], while temporal consistency is governed by the control latency, i.e., the time delay between such transmissions. Both criteria depend on channel access strategy, proximity, and interference, leading to their fundamental trade-offs. Our goal is to develop a tractable framework to jointly analyze controllability and control latency in large-scale wireless control systems.

Several works in the literature study communication–aware control or scheduling [2], [3]. Wang *et al.* [4] demonstrated that accounting for communication disturbances can improve control performance. However, their slot-wise transmissions do not capture block-structured controllability. Recently, communication–control co-design in [1] studies the impact of ALOHA-based channel access on control performance, including learning-based optimization of access parameters. Also, [5] proposes control-aware scheduling policies that adapt based on system state and channel conditions to improve control performance. However, they primarily optimize control performance or learn access policies and do not explicitly characterize temporal consistency in control performance. Overall, prior work [6], [7] remains largely confined to slot-wise or queue-based models, without addressing controllability dynamics. To address these gaps, we consider a network of controller-actuator pairs operating under block-structured transmissions. Controllers are randomly located according to a homogeneous Poisson point process (PPP), and transmit control inputs over an interference-limited wireless channel using block-structured Aloha transmissions. When a transmission fails, control inputs are recomputed. Consequently, controllability requires a minimum run-length of consecutive successful transmissions within each block. For such a system, we jointly analyze and optimize controllability and its temporal evolution, capturing both the probability of achieving controllability and the spacing between controllable events. Our main contributions are as follows:

- We characterize the probability of block controllability, defined as the probability of a predefined number of consecutive successful transmissions within a block, obtained using run-length analysis.
- We capture the temporal reliability of maintaining controllability via peak control latency. It measures the number of blocks elapsed between consecutive controllable blocks, and we derive its distribution and mean.
- We optimize block-access and slot-access probabilities to maximize the probability of achieving controllability while minimizing the peak control latency of the network. Numerical results illustrate the trade-off between controllability and peak control latency, demonstrating the effectiveness of our adaptive access strategy.

II. System Model and Problem Formulation

We consider a shared wireless network that supports multiple controlled systems and their remote controllers. Each controlled system consists of a sensor, a plant, and an actuator. The controller locations are modeled as a homogeneous PPP Φ with density λ. The controller–actuator orientations are assumed to be uniformly at random, forming a Poisson dipole process. The controllers use a reliable link[1] to receive state information at a regular interval of T time slots, referred to as blocks. Then, it calculates control inputs to steer the controlled system to a desired state [1], [5]. These control inputs are transmitted

[1]We assume dedicated resources for the sensor–controller link, since this communication occurs sporadically and involves low payloads, whereas the high-payload control channel is shared.

to the actuator over a shared wireless link, which sends back an acknowledgment. If the acknowledgment is negative, the controller recomputes control inputs and restarts the procedure. The transmission success is determined by signal to interference plus noise ratio (SINR). Since the wireless channel is shared, simultaneous access by all systems would degrade performance. Thus, we adopt a probabilistic channel access protocol to manage transmissions and optimize the SINR and overall control performance. For tractability, we investigate the network from the perspective of the typical controller at the origin, which, by Slivnyak's theorem, does not affect the distribution of the remaining network [8]. To analyze the network, we present the control system model, followed by the transmission model, from this perspective.

A. Control System

The typical controlled system in the network follows a discrete-time linear dynamical system,

$$\mathbf{x}(t+1) = \mathbf{A}\mathbf{x}(t) + \mathbf{B}\mathbf{u}(t) + \mathbf{v}(t), \tag{1}$$

where $\mathbf{x}(t) \in \mathbb{R}^n$ is the state at time slot t, $\mathbf{u}(t) \in \mathbb{R}^m$ is the control input, $\mathbf{v}(t) \in \mathbb{R}^n$ is the zero-mean process noise, and $\mathbf{A} \in \mathbb{R}^{n\times n}$ and $\mathbf{B} \in \mathbb{R}^{n\times m}$ are the the state and input matrices of the system. The system drives and retains the system state at the desired state $\mathbf{x}_{\text{des}}$ with a suitable choice of inputs $\mathbf{u}(t)$.

The controller receives the system state at the beginning of every block, $t = kT$, where block k spans the time slots $t \in \{kT, \ldots, (k+1)T-1\}$. As the process noise $\mathbf{v}(t)$ is zero-mean, it computes a state estimate $\hat{\mathbf{x}}(t)$ for $kT \le t \le (k+1)T-1$ using the received state $\mathbf{x}(kT)$ and (1) as shown in [5], $\hat{\mathbf{x}}(t) = \mathbf{A}^{t-kT}\mathbf{x}(kT) + \sum_{\tau=kT}^{t-1} \mathbf{A}^{t-\tau-1} G(\tau)\mathbf{B}\mathbf{u}(\tau)$, where $G(\tau) \in \{0,1\}$ denotes the transmission acknowledgment sent by the typical actuator to the controller, with $G(\tau) = 1$ indicating successful transmission. At $t = kT$, it designs v control inputs such that $\hat{\mathbf{x}}(t+v) = \mathbf{x}_{\text{des}}$,

$$\left[\mathbf{u}(t)^\top \ \mathbf{u}(t+1)^\top \ldots \mathbf{u}(t+v-1)^\top\right]^\top = \mathbf{\Psi}^\dagger \left[\mathbf{x}_{\text{des}} - \mathbf{A}^v \hat{\mathbf{x}}(t)\right]. \tag{2}$$

Here, v is the controllability index, controllability matrix $\mathbf{\Psi} = \begin{bmatrix}\mathbf{A}^{v-1}\mathbf{B} & \mathbf{A}^{v-2}\mathbf{B} & \ldots & \mathbf{B}\end{bmatrix}$, and $(\cdot)^\dagger$ denotes pseudo-inverse. The controller continues to transmit the control inputs sequentially up to time $kT + l$ until either a transmission fails ($G(kT+l) = 0$) or all v inputs are successfully transmitted ($l = v-1$). If a transmission fails for some $l < v$, the remaining inputs are discarded and a new set of v inputs is recomputed using (2) with $t = kT + l + 1$ and the process repeats. Once v consecutive transmissions succeed, the state estimate $\hat{\mathbf{x}}(t)$ at the controller reaches $\mathbf{x}_{\text{des}}$. After the controller estimate reaches $\mathbf{x}_{\text{des}}$, the actuator applies steady-state inputs till the end of the block to retain the state estimate $\hat{\mathbf{x}}(t)$ at the desired state $\mathbf{x}_{\text{des}}$. These inputs are pre-stored at the actuator and can be computed similarly to (2). However, the steady-state inputs do not account for process noise; applying them alone can lead to unbounded state deviation from $\mathbf{x}_{\text{des}}$ over the full horizon. By recomputing control inputs at the beginning of each block based on the current state, the remote controller compensates for accumulated disturbances, ensuring that the state error remains bounded and grows only proportionally to the block length rather than the entire horizon. Furthermore, after v consecutive successful transmissions, the controller continues transmitting within the block to maintain continuous feedback. These additional dummy packets do not contain control information; however, they allow the actuator to continue sending acknowledgments, supporting interference monitoring and adaptive access control.

B. Propagation Model and Transmission Success

Each wireless link experiences a Rayleigh-distributed fast fading with parameter 1, independent across time and across all links. Let α be the path-loss exponent of each channel, N_{o} be the channel noise power density, and ξ be the transmit power. The SINR $\Upsilon(t)$ at the typical actuator in time slot t is

$$\Upsilon(t) = \frac{\mathbb{I}_o(S_t)\xi \left|h_0(t)\right|^2 r_0^{-\alpha}}{N_o + \sum_{j\in\Phi\setminus\{r_0\}} \mathbb{I}_j(S_t)\xi \left|h_j(t)\right|^2 r_j^{-\alpha}}. \tag{3}$$

where $h_j(t)$ is the channel fading between controller j and the typical actuator. Here, index $j = 0$ denotes the typical controller and r_j denotes the distance between the j-th controller and the typical actuator located at the origin. Also, $\mathbb{I}_j(S_t) \in \{0,1\}$ is the channel access state of controller j at time t where $\mathbb{I}_j(S_t) = 1$ indicates transmission and $\mathbb{I}_j(S_t) = 0$ indicates no transmission. If $\Upsilon(t)$ exceeds a threshold $\gamma > 0$ (depends on the application and receiver hardware), the actuator correctly decodes the received signal, thereby implying a successful transmission. So, the transmission acknowledgment sent by the typical actuator to controller $G(t)$ is 1 (denoting success) if $\mathbb{I}_0(S_t)\Upsilon(t) > \gamma$, and 0 otherwise. We leverage the statistics of the sequence $\{G(t); t \ge 0\}$ to optimize control and latency.

III. Communication-Control Co-design

Our block-structured communication framework prioritizes controllers based on their controllability status to jointly optimize reliability and latency. To this end, we jointly consider two key metrics: block controllability and peak control latency. The controllability is the system's ability to drive its state estimate $\hat{\mathbf{x}}(t)$ to the desired state $\mathbf{x}_{\text{des}}$, which occurs only if v consecutive controller transmissions are successful.

Definition 1 (Controllability)**.** *The typical system is said to be block controllable in block k if there is a run of at least v ones in the sequence $\{G(kT), G(kT+1), \ldots, G((k+1)T-1)\}$.*

While controllability indicates whether control has been achieved in a given block, it does not reflect how frequently it occurs over time. The long-term control reliability is captured by control latency, which measures the number of blocks elapsed since the last controllable block and reflects the temporal consistency of maintaining controllability. The peak control latency is therefore defined with respect to controllable blocks. It quantifies the maximum elapsed time between successive controllable blocks and thus captures the worst-case temporal consistency required to maintain controllability. To formalize this notion, let the indicator variable $\tilde{O}_k = 1$ denote that the typical controller is controllable in block k, and 0 otherwise. The peak control latency is defined as follows.

Definition 2 (Peak control latency)**.** *Suppose block k is controllable, i.e., $\tilde{O}_k = 1$. The peak control latency at block k is defined as $\Theta_k^{\rm pcl} \triangleq \tau$, where $k-\tau$ denote the most recent preceding block*[2] *such that $\tilde{O}_{k-\tau} = 1$.*

Having defined the performance metrics, we next introduce the controller scheduling mechanism. We consider a service horizon of K blocks, each consisting of T time slots. At the beginning of block k, the controller set Φ is partitioned into two disjoint subsets. The set Φ^- contains controllers that have not achieved block controllability up to the end of block $k-1$, while the set $\Phi_{\rm C} \triangleq \Phi \backslash \Phi^-$ consists of those controllers that have. By definition, before the initial block, no controller has yet achieved controllability, and hence $\Phi^- = \Phi$.

To improve the controllability probability for the controllers in Φ^-, we adopt a block Aloha protocol with access probability $\delta_{{\rm B}_k}$. This partitions Φ^- into $\Phi_{\rm B}$, the set of controllers that gain block access, and $\Phi_{\rm S}$, the set of controllers that do not. Controllers in $\Phi_{\rm B}$ access the channel in all slots of block k, whereas the remaining controllers in $\Phi_{\rm S}$ and $\Phi_{\rm C}$ access the channel according to a slotted Aloha protocol with access probabilities $\delta_{{\rm S}_{\rm k}}$ and $\delta_{{\rm C}_{\rm k}}$, respectively. This design prioritizes controllers that have not yet achieved controllability. The probabilistic block access controls the density of always-on transmitters, reducing interference while enabling adaptive scheduling. We optimize these access probabilities $\delta_{{\rm B}_k}, \delta_{{\rm S}_k}$ and $\delta_{{\rm C}_k}$ across blocks to balance the controllability and latency. To establish the optimization formulation, we next analyze the two metrics, connecting them to the access policy.

A. Controllability Analysis

To prioritize controllers that have not yet achieved controllability, we characterize and optimize their controllability probability. Specifically, we derive the block controllability probability, $P_{O_k} \triangleq \mathbb{P}(\tilde{O}_k = 1)$, where the indicator variable $O_k = 1$ denote least one block within $\{1, 2, \ldots, k\}$ has been controllable, i.e., $\tilde{O}_i = 1$ for some $1 \le i \le k$.

The controllers not yet block-controllable form a fraction $1 - P_{{\rm O}_{k-1}}$, while the remaining $P_{{\rm O}_{k-1}}$ are already in the post-controllability regime. Accordingly, the spatial densities $\lambda_{{\rm B}_k}$, $\lambda_{{\rm S}_k}$, and $\lambda_{{\rm C}_k}$ of potentially transmitting controllers in the sets $\Phi_{\rm B}$, $\Phi_{\rm S}$, and $\Phi_{\rm C}$ at block k are given, respectively, by

$$\begin{aligned} &\lambda_{{\rm B}_k} = (1 - P_{{\rm O}_{k-1}})\, \delta_{{\rm B}_k} \lambda \quad \lambda_{{\rm S}_k} = (1 - P_{{\rm O}_{k-1}})(1 - \delta_{{\rm B}_k}) \delta_{{\rm S}_k} \lambda \\ &\lambda_{{\rm C}_k} = P_{{\rm O}_{k-1}}\, \delta_{{\rm C}_k} \lambda. \end{aligned} \tag{4}$$

Here, we start with $\lambda_{{\rm B}_1} = \delta_{{\rm B}_1} \lambda$, $\lambda_{{\rm S}_1} = (1 - \delta_{{\rm B}_1}) \delta_{{\rm S}_1} \lambda$, and $\lambda_{{\rm C}_1} = 0$, as no controller has achieved block controllability before block $k = 1$. Using these densities, the slot-success probability is derived as follows.

Lemma 1. *The conditional slot transmission success probability $\varrho_k = \mathbb{P}(\Upsilon(t) > \gamma \,|\, S_t = 1, \phi)$ of the typical controller in block k is independent of the access mode ϕ and is given by*

$$\varrho_k = \exp\Big(-\frac{\gamma N_o}{\xi r_0^{-\alpha}}\Big) \exp\Big(-2\pi \lambda_{\rm eff} \int_0^\infty \frac{\gamma r^{-\alpha}}{r_0^{-\alpha} + \gamma r^{-\alpha}} r dr\Big),$$

where the parameters ξ, N_0 and α are defined in (3)*, and γ is the SINR threshold for successful transmission, and $\lambda_{\rm eff} = \lambda_{\rm B_k} + \lambda_{\rm S_k} + \lambda_{\rm C_k}$ is the transmitting controller density from* (4)*.*

[2]For consistency in our notations, we define that $\tilde{O}_0 = 1$.

Proof. See Appendix A. □

The next lemma connects the slot-success and controllability probabilities.

Lemma 2. *In block k of T slots, the controllability probability $\mathbb{P}(\tilde{O}_k = 1) = \chi(\mathbb{P}(\Upsilon(t) > \gamma))$ for any slot t in block k, where*

$$\chi(x) = \sum_{l=1}^{\lfloor \frac{T+1}{v+1} \rfloor} (-1)^{l+1} \left[x + \frac{T - lv + 1}{l} (1 - x) \right] \binom{T - lv}{l - 1} x^{lv} (1 - x)^{l-1},$$

where v is the controllability index and γ is the SINR threshold.

Proof. See Appendix B. □

Combining the above two lemmas, we can compute the block controllability probability P_{O_k} recursively as follows.

Theorem 1. *Consider a control network following a PPP with density λ and access probabilities $\delta_{{\rm B}_k}, \delta_{{\rm S}_k}$ and $\delta_{{\rm C}_k}$. The cumulative controllability probability up to block k is*

$$P_{O_k} = P_{O_{k-1}} + (1 - P_{O_{k-1}}) \pi_k, \quad k > 1, \text{ with } P_{O_1} = \pi_1, \tag{5}$$

where π_k is the first-time controllability probability at block k,

$$\pi_k = \mathbb{P}(\tilde{O}_k = 1 \,|\, O_{k-1} = 0) = \delta_{{\rm B}_k} \chi(\varrho_k) + (1 - \delta_{{\rm B}_k}) \chi(\delta_{{\rm S}_k} \varrho_k), \tag{6}$$

where the function $\chi(\cdot)$ is defined in Lemma 2.

Proof. The result follows because $O_k = 1$ if $O_{k-1} = 1$, or if controllability is achieved for the first time in block k. Since these two events are mutually exclusive, we derive (5). Further, to derive (6), we note that conditioned on $O_{k-1} = 0$, the controller belongs to $\phi = \Phi_{\rm B}$ with probability $\delta_{{\rm B}_k}$ or $\phi = \Phi_{\rm S}$ with probability $1 - \delta_{{\rm B}_k}$. Hence, $\pi_k = \delta_{{\rm B}_k} \mathbb{P}(\tilde{O}_k = 1 | O_{k-1} = 0, \phi = \Phi_{\rm B}) + (1 - \delta_{{\rm B}_k}) \mathbb{P}(\tilde{O}_k = 1 | O_{k-1} = 0, \phi = \Phi_{\rm S})$. Now, invoking Lemmas 1 and 2, we arrive at (6). □

B. Peak Control Latency Analysis

The peak control latency of a controllable block is as follows.

Theorem 2. *Consider a control network following a PPP with density λ and access probabilities $\delta_{{\rm B}_k}, \delta_{{\rm S}_k}$ and $\delta_{{\rm C}_k}$. Using ϱ_k and $\chi(\cdot)$ in Lemmas 1 and 2, the peak control latency satisfies*

$$\mathbb{P}(\Theta_k^{\rm pcl} = \tau | \tilde{O}_k = 1) = \frac{P_{\tilde{O}_{k-\tau}} \prod_{i=k-\tau+1}^{k-1} \left(1 - \chi(\delta_{{\rm C}_i} \varrho_i)\right)}{\sum_{\kappa=1}^{k} P_{\tilde{O}_{k-\kappa}} \prod_{i=k-\kappa+1}^{k-1} \left(1 - \chi(\delta_{{\rm C}_i} \varrho_i)\right)}, \tag{7}$$

for $\tau = 1, 2, \ldots, k$. Here, the instantaneous controllability probability $P_{\tilde{O}_k}$ is defined using $P_{O_{k-1}}$ and π_k in Theorem 1 as

$$P_{\tilde{O}_k} = \mathbb{P}(\tilde{O}_k = 1) = (1 - P_{O_{k-1}}) \pi_k + P_{O_{k-1}} \chi(\delta_{{\rm C}_k} \varrho_k). \tag{8}$$

Proof. From Definition 2, for any controllable block k, we get

$$\begin{aligned} &\mathbb{P}(\Theta_k^{\rm pcl} = \tau | \tilde{O}_k = 1) \\ &= \mathbb{P}(\tilde{O}_{k-\tau} = 1, \tilde{O}_{k-\tau+1} = \ldots = \tilde{O}_{k-1} = 0, \tilde{O}_k = 1) / \mathbb{P}(\tilde{O}_k = 1) \end{aligned}$$

$= P_{\tilde{O}_{k-\tau}} \mathbb{P}(\tilde{O}_{k-\tau+1} = \ldots = \tilde{O}_{k-1} = 0, \tilde{O}_k = 1 | \tilde{O}_{k-\tau} = 1) / P_{\tilde{O}_k}$.

If $\tilde{O}_{k-\tau} = 1$, all subsequent blocks $i > k - \tau$ are in the post-controllability regime with slot access δ_{C_i}, implying $\mathbb{P}(\tilde{O}_i = 1 | \tilde{O}_{k-\tau} = 1, \tilde{O}_{k-\tau+1}, \ldots, \tilde{O}_{i-1}) = \chi(\delta_{\mathrm{C}_i} \varrho_i)$. Therefore, using the chain rule, we deduce

$$\mathbb{P}(\Theta_k^{\mathrm{pcl}} = \tau | \tilde{O}_k = 1) = \frac{P_{\tilde{O}_{k-\tau}}}{P_{\tilde{O}_k}} \prod_{i=k-\tau+1}^{k-1} \big(1 - \chi(\delta_{\mathrm{C}_i} \varrho_i)\big) \chi(\delta_{\mathrm{C}_k} \varrho_k),$$

Computing the denominator $P_{\tilde{O}_k}$ from the law of total probability by conditioning on the previous controllable state $k - \kappa$, we derive (7). Then, Theorem 1 implies

$$\begin{aligned} P_{\tilde{O}_k} &= \sum_{o=0,1} \mathbb{P}(O_{k-1} = o) \mathbb{P}(\tilde{O}_k = 1 | O_{k-1} = o) \\ &= (1 - P_{O_{k-1}}) \pi_k + P_{O_{k-1}} \chi(\delta_{\mathrm{C}_k} \varrho_k), \end{aligned}$$

as $\mathbb{P}(\tilde{O}_k = 1 \mid O_{k-1} = 1) = \chi(\delta_{\mathrm{C}_k} \varrho_k)$, deriving (8). □

Using Theorem 2, the expected peak control latency at a controllable block k is

$$\mathbb{E}[\Theta_k^{\mathrm{pcl}} \,|\, \tilde{O}_k = 1] = \frac{\sum_{\tau=1}^{k} \tau P_{\tilde{O}_{k-\tau}} \prod_{i=k-\tau+1}^{k-1} (1 - \chi(\delta_{\mathrm{C}_i} \varrho_i))}{\sum_{\kappa=1}^{k} P_{\tilde{O}_{k-\kappa}} \prod_{i=k-\kappa+1}^{k-1} (1 - \chi(\delta_{\mathrm{C}_i} \varrho_i))}.$$

Building on the controllability and latency analysis, we next formulate the optimization framework for access probabilities.

C. Access Probability Optimization

We optimize access probabilities by balancing two key objectives: minimizing the peak control latency Θ_k^{pcl}, while maximizing the block controllability probability. To make both terms comparable on a probabilistic scale, we express the latency objective via its cumulative distribution function. Therefore, we maximize the following objective function,

$$J(\delta_{\mathrm{B}_k}, \delta_{\mathrm{S}_k}, \delta_{\mathrm{C}_k}) = \rho \, \mathbb{P}(\Theta_k^{\mathrm{pcl}} \leq \eta, \tilde{O}_k = 1) + P_{\mathrm{O}_k},$$

where $\rho \in (0, 1)$ is the regularizer that balances the tradeoff between latency and cumulative controllability. Here, the term P_{O_k} encourages controllers that have not yet achieved controllability to do so, while the first term promotes the likelihood that the peak control latency remains below the threshold η. The first term simplifies as $\mathbb{P}(\Theta_k^{\mathrm{pcl}} \leq \eta, \tilde{O}_k = 1) = \mathbb{P}(\Theta_k^{\mathrm{pcl}} \leq \eta | \tilde{O}_k = 1) P_{\tilde{O}_k}$, where using Theorem 2,

$$\mathbb{P}(\Theta_k^{\mathrm{pcl}} \leq \eta \,|\, \tilde{O}_k = 1) = \frac{\sum_{\tau=1}^{\eta} P_{\tilde{O}_{k-\tau}} \prod_{i=k-\tau+1}^{k-1} \big(1 - \chi(\delta_{\mathrm{C}_i} \varrho_i)\big)}{\sum_{\kappa=1}^{k} P_{\tilde{O}_{k-\kappa}} \prod_{i=k-\kappa+1}^{k-1} \big(1 - \chi(\delta_{\mathrm{C}_i} \varrho_i)\big)}. \tag{9}$$

Therefore, the overall objective function reduces to

$$J(\delta_{\mathrm{B}_k}, \delta_{\mathrm{S}_k}, \delta_{\mathrm{C}_k}) = \rho \, \mathbb{P}(\Theta_k^{\mathrm{pcl}} \leq \eta | \tilde{O}_k = 1) P_{\tilde{O}_k} + P_{\mathrm{O}_k},$$

which is a weighted sum of instantaneous and cumulative controllability probabilities $P_{\tilde{O}_k}$ and P_{O_k} as $\rho \, \mathbb{P}(\Theta_k^{\mathrm{pcl}} \leq \eta | \tilde{O}_k = 1)$ is independent of optimization variables $\delta_{\mathrm{B}_k}, \delta_{\mathrm{S}_k}$ and δ_{C_k}. The resulting optimization problem is nonconvex and admits no closed-form solution; the optimal access probabilities are obtained numerically via an exhaustive grid search over the feasible parameter space.

IV. Numerical Results

In this section, we evaluate our access-policy optimization. The network parameters are set to block length $T = 5$, number of blocks $K = 15$, SINR threshold $\gamma = 0.1$, path-loss exponent $\alpha = 3$, and distance between typical controller and actuator $r_0 = 100$ m. The transmit power $P = 40$ dBm, noise power $N_0 = 10^{-17}$, latency threshold $\eta = 3$, and weight $\rho = 0.8$. The access probabilities are obtained via exhaustive grid search over $[0, 1]^3$. Fig. 1 shows the optimized policies and resulting controllability for PPP density $\lambda \in \{1 \times 10^{-4}, 1.5 \times 10^{-4}\}$ and controllability index $v \in \{2, 3\}$, highlighting the tradeoff between controllability, interference, and latency.

In Fig. 1(a), with $v = 2$ and $\lambda = 10^{-4}$, controllability is achieved rapidly, as only two consecutive successes are required. Accordingly, δ_{B_k} increases from 0.45 to 1 by $k = 3$ and then drops to zero. Then, the policy switches to $\delta_{S_k} = 1$ at $k = 4$ and P_{O_k} reaches unity at the same step. Thereafter, all controllers belong to Φ_{C} and the policy stabilizes with δ_{C_k} around 0.62. In this regime, no controller is prioritized and thus, $P_{\tilde{O}_k}$ decreases due to fewer new controllability events.

In Fig. 1(b), with higher density $\lambda = 1.5 \times 10^{-4}$, increased interference reduces access probabilities compared to Fig. 1(a). Here, δ_{B_k} peaks at 0.7 at $k = 4$ before dropping to zero, the transition to $\delta_{S_k} = 1$ occurs at $k = 5$, and δ_{C_k} stabilizes near 0.42 after $k = 6$. As a result, P_{O_k} reaches unity later than Fig. 1(a), around $k = 6$, while $P_{\tilde{O}_k}$ reduces to 0.1 due to the reduced likelihood of successful transmission runs.

In Fig. 1(c), for $v = 3$ and $\lambda = 10^{-4}$, longer success runs are required, making it harder to achieve controllability. Thus, δ_{B_k} increases more gradually and persists longer, with a delayed transition to slot access compared to Fig. 1(a). The cumulative controllability P_{O_k} approaches unity only around $k = 9$, while $P_{\tilde{O}_k}$ remains low for most of the horizon.

Fig. 1(d) shows the most challenging case, with $v = 3$ and $\lambda = 1.5 \times 10^{-4}$. Here, both the stricter controllability requirement and the stronger interference slow the evolution of the access policy. The block-access probability δ_{B_k} starts from a low value and increases steadily until $k = 10$, before dropping sharply. The slot-access probability δ_{S_k} remains zero for longer till $k = 10$ and becomes unity for $k \geq 11$. The post-controllability probability δ_{C_k} appears only toward the end of the horizon, where additional transmissions are used to support controllability while respecting the latency objective. Accordingly, P_{O_k} increases much more slowly than in the other cases and reaches unity only near the end of the time horizon, while $P_{\tilde{O}_k}$ stays low throughout most of the evolution.

Overall, the results show that smaller values of v enable faster controllability, whereas higher controller density λ delays it. The optimized access policy handles this by allocating early block access and progressively shifting to slot access once controllability is achieved.

V. Conclusion

This paper studied a communication-control co-design framework for wireless networked control systems with block

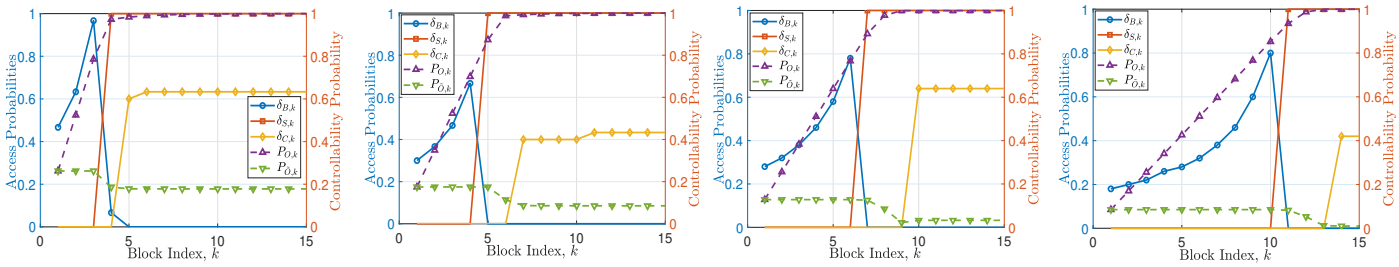

(a) $v = 2, \lambda = 1 \times 10^{-4}$ (b) $v = 2, \lambda = 1.5 \times 10^{-4}$ (c) $v = 3, \lambda = 1 \times 10^{-4}$ (d) $v = 3, \lambda = 1.5 \times 10^{-4}$

Figure 1: Evolution of access probabilities and controllability performance as a function of block index k with $T = 5$.

transmissions, modeling controllers as a spatial PPP. We analyzed the impact of probabilistic channel access on controllability and latency. Based on these analytical results, we optimized the access probabilities to balance controllability and peak control latency. Numerical results demonstrated that adaptive block- and slot-based access policies improve reliability while controlling latency in large-scale wireless control networks. Future work can consider extensions to networks with heterogeneous controllers and learning-based adaptive access schemes.

Appendix A

Proof of Lemma 1 : For any ϕ, the set of interfering controllers is $\bar{\Phi}_t = \{j \in \Phi_{\mathrm{B}} \cup \Phi_{\mathrm{S}} \cup \Phi_{\mathrm{C}} \setminus \{0\} : \mathbb{I}_j(S_t) = 1\}$. Here, the indicator $\mathbb{I}_j(S_t) = 1$ if controller j transmits in slot t. The process $\bar{\Phi}_t$ follows a PPP with density λ_{eff}. Now, using (3), we deduce

$$\varrho_k = \mathbb{P}\left(\frac{\xi|h_0(t)|^2 r_0^{-\alpha}}{N_o + \sum_{j\in\bar{\Phi}_t} \xi|h_j(t)|^2 r_j^{-\alpha}} > \gamma\right)$$
$$= \exp\left(-\frac{\gamma N_o}{\xi r_0^{-\alpha}}\right) \mathbb{E}\left[e^{-\sum_{j\in\bar{\Phi}_t} |h_j(t)|^2 \gamma \frac{r_j^{-\alpha}}{r_0^{-\alpha}}}\right]$$

because $|h_0(t)|^2 \sim \exp(1)$. Since $|h_j(t)|^2 \gamma \frac{r_j^{-\alpha}}{r_0^{-\alpha}} \sim \exp\left(\frac{r_0^{-\alpha}}{\gamma r_j^{-\alpha}}\right)$, and $\bar{\Phi}_t$ follows a PPP with density λ_{eff}, we simplify the above expression by applying probability generating functions [9] to obtain the desired result.

Appendix B

Proof of Lemma 2 : It suffices to show that $\chi(x)$ is the probability that a Bernoulli sequence $\{Y(t) \in \{0,1\}\}_{t=1}^{T}$ with mean x contains a run of at least v ones. For $i' = 1, 2, \ldots, T-v+1$, we define the event $\mathcal{A}_{i'} \triangleq \{Y(i') = Y(i'+1) = \cdots = Y(i'+v-1) = 1\}$, corresponding to a run of v consecutive successes starting at slot i'. Then, $\chi(x) = \mathbb{P}\left(\bigcup_{i'=1}^{T-v+1} \mathcal{A}_{i'}\right)$. Simply summing the probabilities $\mathbb{P}(A_{i'})$ overcounts outcomes with multiple runs. By the principle of inclusion-exclusion,

$$\chi(x) = \sum_{l=1}^{T-v+1} (-1)^{l+1} \sum_{1\le i'_1<\cdots<i'_l\le T-v+1} \mathbb{P}(A_{i'_1} \cap \cdots \cap A_{i'_l}). \quad (10)$$

The first term $(l = 1)$ adds the probabilities of individual runs. The second term $(l = 2)$ subtracts the probabilities of pairs of runs that occur together, correcting for double counting. Higher-order terms alternately add and subtract probabilities of three or more simultaneous runs. To ensure l runs of length v are distinct and non-overlapping, at least one empty slot must separate consecutive runs. Thus, $(l-1)$ gaps are needed among lv occupied slots, so $lv + (l-1) \le T$, which gives $l \le \left\lfloor \frac{T+1}{v+1} \right\rfloor$. For any admissible selection of l nonoverlapping runs, the joint probability that all l runs occur is $\mathbb{P}(A_{i'_1} \cap \cdots \cap A_{i'_l}) = x^{lv}(1-x)^{l-1}$, where x^{lv} accounts for the lv successful slots within the runs, and $(1-x)^{l-1}$ ensures separation between consecutive runs. After allocating lv slots to the runs, the remaining $T - lv$ slots can be distributed among the $(l-1)$ separating gaps, yielding $\binom{T-lv}{l-1}$ admissible placements. Runs starting at the first slot or ending at the last slot create boundary effects because they need a separating failure on only one side, whereas interior runs require failures on both sides. In line with classical run distributions (e.g., de Moivre's run problem), this yields the correction factor $x + \frac{T-lv+1}{l}(1-x)$, where X_k accounts for boundary-attached runs (those starting at the first slot or ending at the last slot). The term $\frac{T-lv+1}{l}(1-x)$ accounts for interior runs: $T-lv+1$ is the number of admissible starting positions, division by l averages over the l runs, and $(1-x)$ enforces a separating failure. Substituting this into (10) and $\mathbb{P}(A_{i'_1} \cap \cdots \cap A_{i'_l})$ expression yields Lemma 2.

References

[1] G. Ghatak, G. Joseph, and C. Quan, "Channel access strategies for control–communication co-designed networks," *IEEE Trans. on Control of Netw. Syst.*, vol. 13, no. 1, pp. 117–129, 2026.

[2] S. Das and G. Ghatak, "A stochastic geometry analysis of energy-age tradeoff in wireless IoT network," in *Proc. WiOpt workshop RAWNET*, 2024, pp. 46–53.

[3] ——, "Analysis of age-energy trade-off in IoT networks using stochastic geometry," *IEEE Trans. Green Commun. Netw.*, vol. 10, pp. 236–248, 2026.

[4] X. Wang, C. Chen, J. He, S. Zhu, and X. Guan, "AoI-aware control and communication co-design for industrial IoT systems," *IEEE Internet Things J.*, vol. 8, no. 10, pp. 8464–8473, 2021.

[5] G. Ghatak, G. Joseph, and C. Quan, "Poisson Networked Control Systems: Statistical Analysis and Online Learning for Channel Access," in *Proc. WiOpt workshop RAWNET*, 2024, pp. 62–69.

[6] Y. Qiao, Y. Fu, and M. Yuan, "Communication–control co-design in wireless networks: A cloud control AGV example," *IEEE Internet Things J.*, vol. 10, no. 3, pp. 2346–2359, 2023.

[7] Y. Wang *et al.*, "A review on wireless networked control system: The communication perspective," *IEEE Internet Things J.*, vol. 11, no. 5, pp. 7499–7524, 2024.

[8] S. N. Chiu *et al.*, *Stochastic geometry and its applications*. John Wiley & Sons, 2013.

[9] P. D. Mankar, H. S. Dhillon, and M. Haenggi, "Meta distribution analysis of the downlink SIR for the typical cell in a Poisson cellular network," in *IEEE Glob. Commun. Conf. (GLOBECOM)*, 2019, pp. 1–6.